4.3 PREPARATION FOR THE ASSIMILATION OF ADVANCED SOUNDERS AT METEO-FRANCE

Florence Rabier *, Nadia Fourrié, Thomas Auligné
Météo-France, Toulouse, France
Malgorzata Szczech-Gajewska
IMWM, Krakow,Poland

1 INTRODUCTION

By measuring radiation in thousands of different channels, advanced infrared sounders such as the Atmospheric InfraRed Sounder (AIRS, 2378 channels) and the Infrared Atmospheric Sounding Interferometer (IASI, 8461 channels) have the potential to provide atmospheric temperature and composition information at a much higher vertical resolution and accuracy that can be achieved with the current generation of operational sounding instruments. The successful exploitation of these next generation of satellite instruments is one of the major challenges for Numerical Weather Prediction (NWP) centres in the next decade.

However, it is neither feasible nor efficient to assimilate all of the channels and a policy of data compression such as channel selection has to be designed in the context of NWP. The challenge is to find a set of channels that is small enough to be assimilated efficiently in a global NWP system (with operational time constraints) but which is still large enough to capture important atmospheric variability.

Rabier et al. (2002) have investigated the possibilities of choosing an "optimal" subset of data for the IASI interferometer. These issues have been addressed in the context of optimal linear estimation theory, using simulated data. Several methods have been tried to select a set of the most useful channels for each individual atmospheric profile. An iterative method selecting sequentially the channels with largest information content was demonstrated to always produce the best results, but at a relatively large cost. To test the robustness of this iterative method, a variant has been tried. It consists in building a mean channel selection aimed at optimizing the results over the whole profile database, and then applying to each profile this "constant" selection. Results show that this "constant" iterative method is very promising. The practical advantage of this method for operational purposes is that the same set of channels can be used for various atmospheric profiles. Results are presented in section 2. Following the launch of the NASA[1] AQUA satellite in May 2002, a reduced set of AIRS radiance channels will be made available to the scientific community in Near Real Time (NRT) by NOAA[2]/NESDIS[3] and NWP centres are planning to exploit this reduced set at day one. The main goal of Fourrié and Thépaut (2002) is to apply Rabier et al. (2002) methodology to the AIRS instrument in order to assess the quality of the NRT NESDIS channel selection versus a more optimal channel selection. This approach has been applied to simulated AIRS data. Results show that, although the "constant" channel selection is significantly different from the one used by NESDIS for the distribution of AIRS data to NWP centres, results in terms of retrieval accuracy are very similar as shown in section 3. These channel selection studies apply to clear-sky conditions and have to be extended to cloudy conditions. In order to address the question of cloudiness in sensitive areas, eight FASTEX (Fronts and Atlantic Storm-Track Experiment) cases in February 1997 have been studied. Sensitive areas are regions where small errors in the initial conditions can lead to large forecast errors. In every sounder pixel, cloud parameters were deduced from the AVHRR (Advanced Very High Resolution Radiometer) observations with the MAIA algorithm (Mask AVHRR for ATOVS Inversion). Results show that most of the sensitive area is covered with clouds. High clouds are mostly located in the southern part of

* Corresponding author address : CNRM/GMAP, Météo-France, 42 av. G. Coriolis, F-31057 Toulouse Cedex, email=florence.rabier@meteo.fr

[1] National Aeronautic and Space Agency
[2] National Oceanic and Atmospheric Administration
[3] National Environmental Satellite Data and Infomation Service

the sensitive area, while low clouds predominantly affect the northern part. Section 4 illustrates the main results of this study. In parallel, the assimilation of advanced sounder data over land is being prepared. Spectrally varying emissivities are computed for each soil type used as climatological input to the NWP model. The spectral variation is presented in section 5. This preparation for advanced sounder data has been performed using mainly AIRS and IASI simulated data. As AIRS data become available, we intend to start monitoring the radiance data and revisit the subject with real statistics. First results with the very first day of AIRS data available at NWP centres are shown in section 6. Section 7 concludes this presentation.

2 CHOICE OF A CHANNEL SELECTION FOR IASI

2.1 Experimental framework

The general framework of this study is the linear optimal estimation theory in the context of NWP. The optimal analysed state x_a is given by $x_a = x_b + \mathbf{K}(y - y_b)$, with x_b the background vector state, $\mathbf{K} = \mathbf{A}\mathbf{H}^\top\mathbf{R}^{-1}$, y the observation state, $y_b = \mathbf{H}x_b$. $\mathbf{H}$ is the tangent linear of the radiative transfer operator $\mathcal{H}$ ($\mathcal{H}(x) = \mathcal{H}(x_b) + \mathbf{H}(x - x_b)$). $\mathbf{A} = (\mathbf{B}^{-1} + \mathbf{H}^\top\mathbf{R}^{-1}\mathbf{H})^{-1}$ is the analysis error covariance matrix. $\mathbf{R}$ is the observation error covariance matrix and $\mathbf{B}$ is the background error covariance matrix.

Some useful information theory concepts can be used to quantify the gain in information brought by the data. These are in particular the Degrees of Freedom Signal (DFS): $\mathrm{DFS} = \mathrm{Tr}\left(\mathbf{I} - \mathbf{A}\mathbf{B}^{-1}\right)$, or the Entropy Reduction (ER): $\mathrm{ER} = -\frac{1}{2}\log_2 det(\mathbf{A}\mathbf{B}^{-1})$. Both quantities give a global measure of the reduction of uncertainty brought by the analysis as explained in Rodgers (2000). For more detailed diagnostics of the quality of the analysis, one can use the standard-deviations of analysis errors (from the diagonal components of $\mathbf{A}$).

For this study we have used a set of 492 representative atmospheric profiles (temperature and humidity). IASI data have been simulated from each profile, using the fast radiative transfer model RTIASI (Matricardi and Saunders, 1999) over sea with a nadir-viewing angle, the scene being assumed to be cloud-free. The parameters to be retrieved are the temperature and the humidity profiles over the 43 RTIASI levels. The background error covariance matrix is typical of a state of art NWP model and has been built from the 60 level ECMWF covariance matrix representing short-range forecast errors.

2.2 Results

Several channel selection methods were tried. For more details about the description of the methods tested is this study, see Rabier et al. (2002). The most successful is found to be an iterative method based on Rodgers (1996) which consists in performing a series of successive analyses, each one using only one additional channel optimizing the ER at a time. At each step, the analysis error covariance matrix is updated and it will be used at the next step. It is interesting to illustrate the variation of analysis quality when the number of selected channels is varied from less than 100 to 8461. Results are shown in Fig. 1 for the analysis error standard-deviations (averaged over 24 mid-latitude profiles). The gain brought by the first 86 channels is remarkable compared to the background. Increasing the number of channels gradually increases the information content and analysis quality. This improvement in analysis quality is more obvious in the tropospheric temperature than in the stratospheric temperature, and very significant in the lower humidity profile (not shown). Although 300 channels provide a considerable achievement in terms of analysis quality compared to what can be expected from other instruments, it is obvious that the information content has not yet reached an asymptotic value and one would benefit from using at least up to 2000 channels. For instance, going from 300 to 8461 channels brings a decrease in maximum error in the tropospheric temperature profile from 1.5K to 1K, and in the humidity profile from 0.6 g/kg to 0.4 g/kg (not shown). Similarly, the vertical resolution typical for temperature and humidity is improved from around 2km to 1.5km (not shown). One should note that these results are very dependent on the background error covariance matrix $\mathbf{B}$ used in this study, and cannot be compared easily to other results using very different background information.

For an operational assimilation system, the selection of 300 channels per IASI pixel is assumed to be tractable. However, the cost of performing the choice of 300 channels at each location is not negligible. If one considers that the iterative method is too expensive to be performed for each atmospheric profile, one might consider one solution: a "constant" selection based on off-line studies with the iterative method.

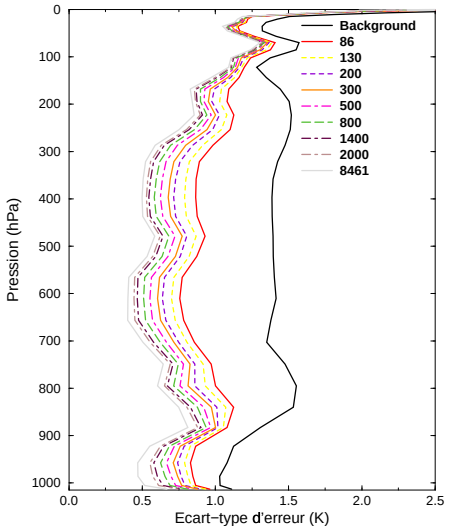

Figure 1: Standard-deviation of temperature analysis errors averaged over 24 mid-latitude profiles, for various number of channels selected with the iterative method.

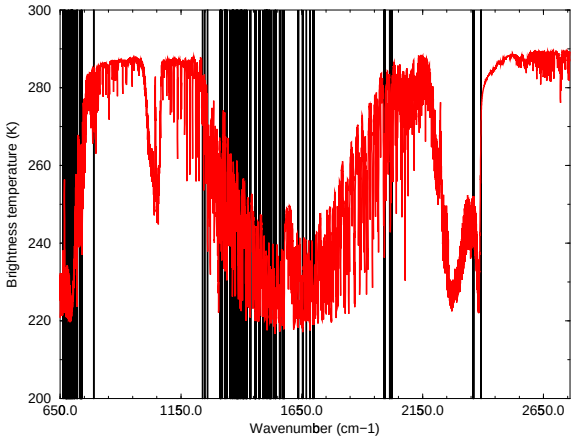

Figure 2: Location of the 300 channels selected for the retrieval of temperature and humidity by the "constant" iterative method for IASI.

Firstly a constant channel selection is computed from a set of 492 different channel selection (corresponding to our database of representative atmospheric profiles) provided by the iterative method. For each selection, one assigns a rank from 1 to 300 to each channel picked by the iterative selection, all the others having the largest possible rank corresponding to the number of channels on which the selection is performed. Then channels are selected according to their lower average rank, by increasing order.

When applying this constant selection (presented in Figure 2) to the whole set of profiles, one loses around 0.7 units in terms of DFS compared to the optimal selection varying with each profile. This is considered to be a negligible loss. In any case, this "constant" channel selection still proved to be better than other methods tried in Rabier et al. (2002).

3 APPLICATION OF THIS CHANNEL SELECTION TO AIRS

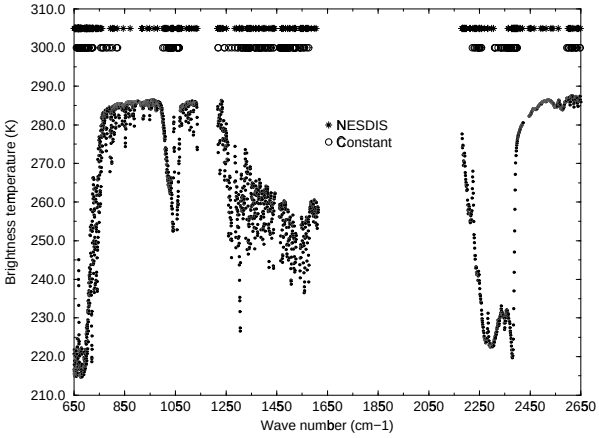

Figure 3: Typical spectrum of AIRS and location of the channels selected by the NESDIS NRT set and the constant iterative method.

Following the launch of the NASA[4] AQUA satellite in May 2002, a reduced set of AIRS radiance channels will be made available to the scientific community in Near Real Time (NRT) by NOAA[5]/NESDIS[6] and

[4] National Aeronautic and Space Agency
[5] National Oceanic and Atmospheric Administration
[6] National Environmental Satellite Data and Infomation Service

NWP centres are planning to exploit this reduced set at day one.

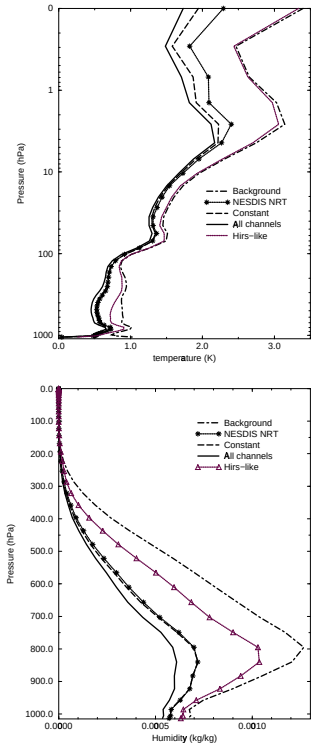

Figure 4: Standard-deviation of errors averaged over 108 profiles, for various channel selections to retrieve temperature (top panel), humidity (bottom panel) and ozone (Fig. 4 continued). 'Background' corresponds to the standard deviation of background errors. 'Nesdis NRT' and 'constant' are related to the standard deviation of analysis errors obtained with the NESDIS Near Real Time set and constant set. 'All channels' corresponds to the standard deviation obtained with an analysis using all AIRS channels. 'Hirs-like' corresponds to the standard deviation obtained with an analysis using 15 AIRS channels corresponding to the current High-resolution Infrared Radiation Sounder.

As seen in the previous section, Rabier et al. (2002) have tested several methods and found that the most suitable is a method following Rodgers (1996) reducing the number of IASI channels (in clear sky conditions) in an optimal way which preserves the information content of the instrument. The main goal of the study described in this section (performed at ECMWF, Fourrié and Thépaut, 2002) is to apply

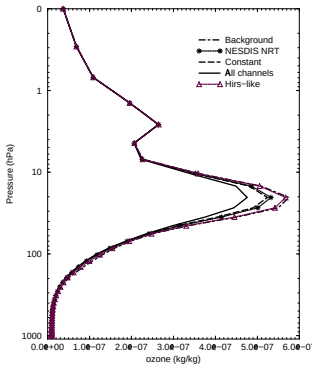

Fig. 4 continued.

Rabier et al. (2002) methodology to the AIRS instrument in order to assess the quality of the NRT NESDIS channel selection versus one based on optimal information content. In this study, the background fields and the AIRS data have been simulated from a set of representative atmospheric situations. This set is part of the ECMWF atmospheric data base (Chevallier et al., 2000) and forms a set of 108 profiles of temperature, humidity, ozone, surface temperature and surface pressure covering most of atmospheric variability. All atmospheric scenes are assumed to be cloud-free, over sea and for nadir views. The 108 profiles are divided into 75 midlatitude (20N-70N,20S-70S), 14 tropical (20N-20S) and 19 polar (70N- 90N, 70S-90S) profiles. As a starting point, we have considered the fact that 324 channels will be available in the NESDIS NRT dataset. Since some channels are known to be of less good quality, we have excluded the channels whose quality rating flag does not correspond to a good quality flag. Applying this check, the total number of AIRS channels is reduced from 2378 to 2140. For these experiments a more recent version of the background error covariance matrix has been used.

As pointed out by Rabier et al. (2002), the iterative method if applied bluntly (one optimal channel selection per atmospheric profile) can be very CPU time consuming and would certainly be impossible to apply in an operational context. Therefore a constant channel selection of 324 channels has been computed as an average selection based on the set of 108 different optimal channel selections (one per atmospheric profile). This average selection will be called thereafter "constant" and will be compared with the NESDIS NRT selection. Worth mentioning is that only

63 channels are always selected throughout the 108 channel selections (corresponding to very different atmospheric situations), whereas 1504 channels are never selected. The resulting constant channel selection shares 119 channels with NESDIS NRT selection. Figure 3 displays the AIRS spectrum corresponding to a midlatitude profile with the location of the NESDIS NRT selected channels (stars) and constant channel selection (circles). At first sight, the NESDIS NRT channel set spans more evenly the IR spectrum than the constant channel set which focusses more on specific small spectral domains. 53% of NESDIS NRT channels are located in the 649-1150 cm^{-1} (longwave and ozone) band againt 36% of the constant channels while 40% of this latter set are chosen in the 1150-1650 cm^{-1} (water vapour) band. The 4.5 μm band is hardly covered by the constant channel selection, whereas both NESDIS NRT and constant channels describe evenly the 4.2 μm $CO_2$2 band. The ozone band (1050 cm^{-1}) is also well captured by the two selections. The study of the jacobians of the channels exclusively selected by NESDIS NRT and constant (not shown) indicates an overrepresentation of the upper stratosphere and the dominating choice of the water vapour band in the constant channel selection, partly driven by the vertical structure of the humidity background error covariance matrix. The overrepresentation of the upper-stratosphere can be also explained by the large background error variances at upper levels. The corresponding channels are located in the CO_2 band at around 2350 cm^{-1}. Conversely, NESDIS NRT has a large number of channels peaking in the low troposphere corresponding to the 650-750 cm^{-1} band and to the 2400-2600 cm^{-1} band.

When looking at the "efficiency" of both channel selections (not shown), the ER and DFS are found to be slightly smaller for the NESDIS NRT selection (49.93 versus 57.94 and 18.36 versus 20.59 respectively). However, these two selections greatly improve the DFS and the ER compared to the use of the 15 channels correponding to the current High-resolution Infrared Radiation Sounder (14.06 for ER and 6.44 for DFS). The standard deviations of the background error and of the linear 1D-Var analysis error have then been studied for temperature, humidity and ozone parameters as well as the surface temperature, for all the 108 profiles (Figure 4). Firstly, the NESDIS NRT and the constant selection reduce the analysis error in temperature, humidity and ozone compared to the "HIRS-like" set. The NESDIS NRT and the constant selection provide similar temperature retrieval errors in the lower troposphere, while the constant selection gives analysis errors in general smaller than 2 K in the upper-troposphere and in the stratosphere (versus 2.5 K or more with the NESDIS NRT selection). In addition, the NESDIS NRT and constant selections provide similar humidity and ozone analysis errors.

For surface temperature, the analysis error standard deviation is decreased to 0.05 K for both selections instead of 1.02 K for the background and 0.3 K for the "HIRS-like" channel set. The very low values of analysis error standard deviation can be explained by the fact that the background error is not very well known for the surface temperature and not well specified in the $\mathbf{B}$ matrix and by the assumed perfect emissivity.

Comparisons with retrieval errors using all the AIRS channels (Fig. 4) show that these additional channels lead to a further reduction of temperature analysis error of about 0.1 K in the troposphere and roughly of 0.2 K in the stratosphere. The improvement in the humidity analysis is also very large in the lower troposphere when all the channels are used in the assimilation. Likewise, the ozone retrieval error is largely decreased when the 2378 channels are used. The further gain in ER and in DFS is 18.2 and 3.75 respectively when the 2378 channels are used in the analysis.

In conclusion, if a loss of information content is to be expected by using around one tenth of the total number of AIRS channels, the NESDIS NRT selection seems reasonable for NWP applications. Even though the information content is slightly smaller than for the constant selection, the respective performance of NESDIS NRT and constant selections is very comparable in terms of linear 1D-Var retrieval error (and this applies for temperature, humidity, ozone and surface temperature).

4 SENSITIVE AREAS AND CLOUDS

If advanced sounders have to lead to a very significant impact on the forecast quality, one should address in details the question of retaining the most information possible in the sensitive areas. Previous studies such as those of Prunet et al (1998) and Collard (1998) have suggested that IASI could resolve some of the small scale baroclinic structures that have been identified by the sensitivity studies as being crucial to forecast error development (Rabier et al., 1996). The main obstacle to use informa-

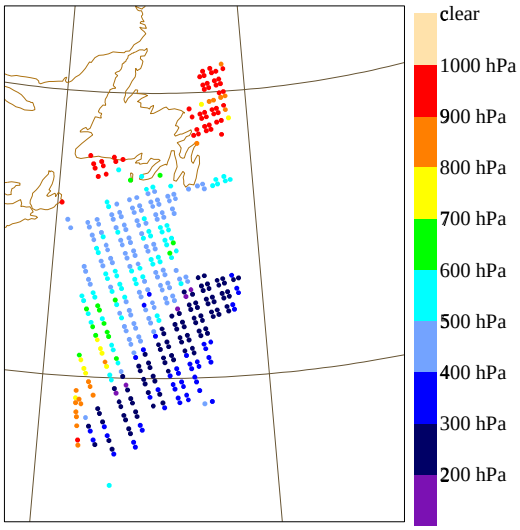

Figure 5: Distribution of the cloud top pressure of the IASI pixels for the sensitive area, for the IOP 17 (18th February 1997 at 0UTC). The graduation varies from 200 to 1000hPa and cream dots correspond to clear sky pixels.

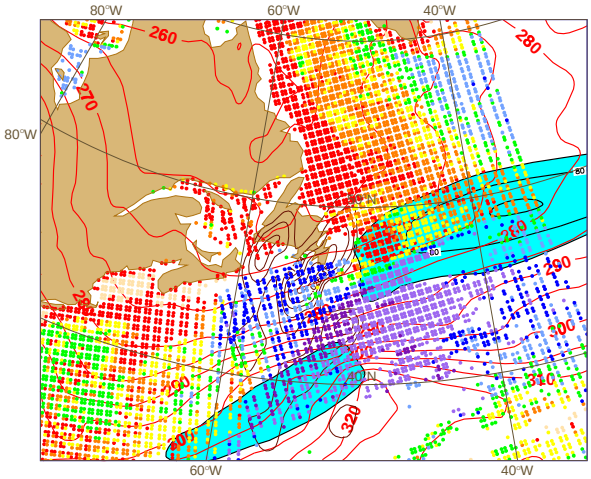

Figure 6: Distribution of the cloud top pressure of the IASI pixels for the whole area for the IOP17. The blue shaded area corresponds to the 300hPa wind velocity above 60m/s. The red lines represent the 850hPa equivalent potential temperature.

tion from advanced sounders is the presence of cloud which can severely limit the information from infrared sounders. In this context, McNally (2000) previously investigated the occurrence of clouds in the sensitive areas with cloud fields from the ECMWF model and showed with an "observable" sensitivity variable that there was a high correlation between the meteolorogically sensitive areas and the cloud cover produced by the ECMWF model. The first objective of this study is also to establish the cloud cover and the cloud top level for meteorological situations over the North Atlantic Ocean, and more particularly in the sensitive areas for the forecasts of storms during the FASTEX (Front and Atlantic Storm-Track Experiment, Joly et al., 1999) experiment.

This section presents the study of the cloudiness in the meteorological sensitive areas. The cloud study is performed using cloud parameters derived from the satellite imager AVHRR (in constrast to Mc Nally's study). In this study the cloud parameters (cloud cover in IASI pixel and cloud top pressure) have been retrieved from the AVHRR imager using the MAIA (Mask AVHRR for Inversion ATOVS) method which was originally developed at the CMS [7] in the frame of the AVHRR and ATOVS Processing Package (Lavanant et al., 1999). Originally the MAIA method was developped for the inversion of ATOVS observations. Then it was adapted to the IASI observations (Lavanant, pers comm). It processes the AVHRR pixels mapped inside the simulated IASI field of view and determines the mean clear percentage cover in the IASI spot. With a succession of thresholds tests applied to AVHRR channels inside the simulated IASI pixel it is possible to determine some cloud parameters. The percentage of clear AVHRR spots in the IASI pixel and, for the cloudy pixels, the cloud top temperature (if the cloud can be considered as a black body) among other parameters are available as outputs of the MAIA algorithm. The cloud cover is evaluated from the percentage of clear AVHRR pixels in each simulated IASI ellipse shape.

A minimum threshold of 90% of clear AVHRR spots present in the IASI pixel has been arbitrarily chosen in order to consider this IASI pixel as clear. For cloudy pixels, the cloud top pressure level is determined from the cloud top temperature with a series of differences between the cloud top temperature from the MAIA method and the analysis temperature profile interpolated onto the simulated observation location. The temperature fields are available at every 50 hPa in the vertical and are provided by the 4D-Var reanalysis of the FASTEX experiment (Desroziers

[7] Centre de Météorologie Spatiale

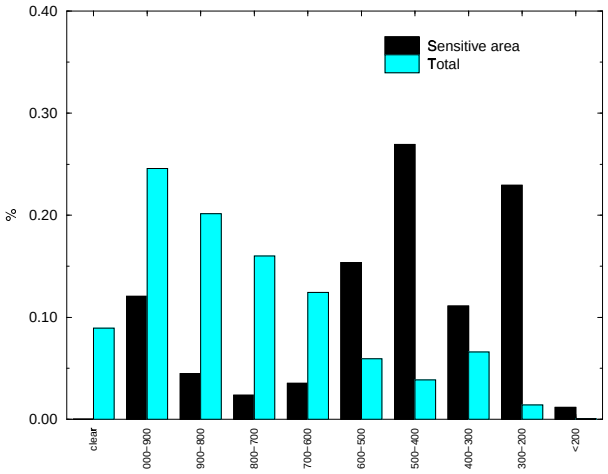

Figure 7: Distribution (percentage) of the cloud top level of the IASI pixels averaged over the sensitive area of the FASTEX Intensive Observing Period 17 and the whole data set corresponding to a mid-latitude region.

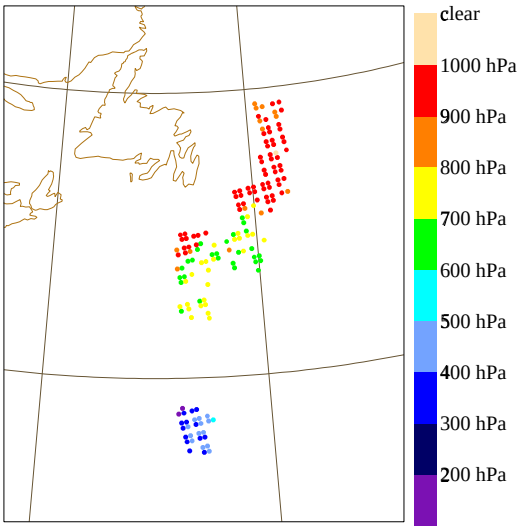

Figure 8: Distribution of the cloud top pressure of the IASI pixels for the sensitive area, for the 26th February 1997 at 0UTC. of the IASI pixels for the sensitive area.

et al., 2002). The cloud top pressure level is found when the difference between the cloud top temperature and the atmospheric profile is the smallest as possible. It is worthwhile to note that only pixels over the sea have been considered in this study. Indeed, the method having been mainly tested over ocean owing to the CMS reception area, there is a lack of confidence in the method over iced land surfaces. Short-term forecast errors are mainly due to errors in the forecast initial state. In order to determine the region where small errors in the initial state may increase and lead to major forecast errors, one can use the gradient of a diagnostic function of the final state with respect to the initial conditions (Rabier et al., 1996). Sensitive areas have been defined with scaled gradients fields resulting from adjoint calculations. In this study, the gradient is based on the diagnostic function of the Hello et al. (2000) study. It is computed from the forecast of the mean sea level pressure over the area of the considered FASTEX weather systems. Eight dates spanning the month of February 1997 have been studied. This period corresponds to a zonal weather regime, which is favourable to the development of cyclonic systems over western Europe.

The temperature fields of the gradient at 900, 800, 700, 600 and 500 hPa levels have been considered: they have been squared and summed at each geographical location in order to obtain a single horizontal sensitivity field. Once the sensitivity field has been computed, we apply a threshold (arbitrarily fixed at 30% of the largest sensitivity field value) to this field in order to obtain an horizontal mask for the observations located in a sensitive area for which we will study the cloud cover and the cloud top height.

Before presenting the overall results for the 8 IOPs, a single case, the "FASTEX cyclone", is more especially studied in the next subsection.

4.1 A case study: the FASTEX Intensive Observing Period 17

The considered case study is the FASTEX IOP 17 which is a well sampled case. It is an example of a complex life-cycle low ending as an explosive cyclogenesis at 00 UTC 20 february 1997, with a strong deepening rate of 40 hPa in 24 hours and a lowest central pressure of 943 hPa. The considered analysis is made at 00 UTC 18 February and the subsequent forecast range is 36 hours. The verification area is included in the region [63N, 5 2N; 20W, 0W] on 12 UTC 19 February 1997. The sensitive area is located above and south Newfoundland (Fig. 5). Figure 5 displays the cloud top pressure of the 423 simulated IASI pixels located in the sensitive area. A

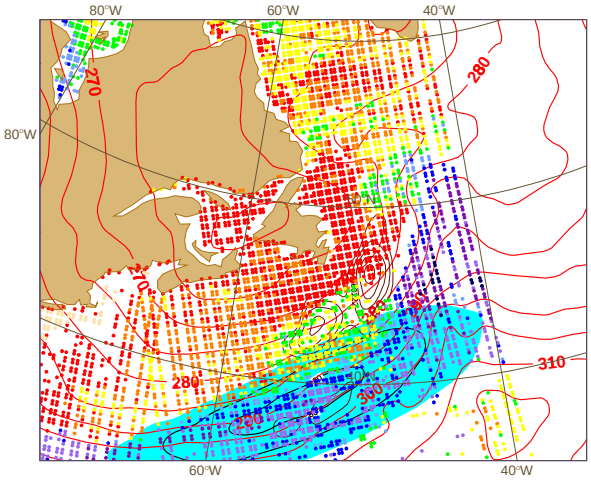

Figure 9: Distribution of the cloud top pressure of the IASI pixels for the whole area for the IOP19.

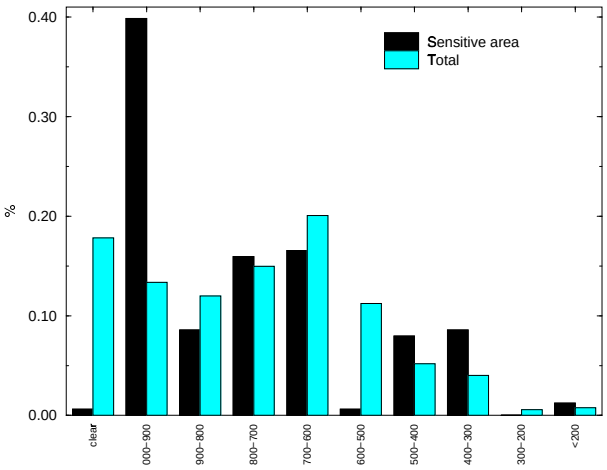

Figure 10: Distribution of the cloud top level of the IASI pixels averaged over the sensitive area and the whole data set corresponding to a mid-latitude re gion for the IOP19.

large amount of cloud top pressure above 600 hPa is observed in the southern part of the sensitive area even though low-level clouds are present in its northern part. This particular distribution of clouds can be explained by the meteorological situation (Fig. 6). Indeed, the sensitive area is located in-between two upper-level jets and a so-called cloud head pattern with high-level cloud has developed. This cloud is indicative of a rapid cyclogenesis. The corresponding distribution of the cloud top pressure is exhibited in Figure 7. The blue bars are representative of the observation data set over a large mid-latitude region while the black bars corresponds to the observations located in the sensitive area. As already mentioned, a large part of the clouds have top pressure level above 600 hPa (more than 75%) and the low-level clouds of the northern part of the sensitive area represent 12% of the clouds. On the contrary, the clouds observed in the whole data set are mainly low-level clouds and very few clouds are located above 500 hPa. In addition, almost 10% of simulated IASI pixels are cloud-free.

4.2 A case study: the FASTEX Intensive Observing Period 19

The analysis is made at 0 UTC 26 February and the subsequent forecast range is 36 hours. The verification area is included in the region [63.5N 57N; 30W, 13W] on 12 UTC 27 February. The sensitivity maximum is located at 800 hPa. Figure 8 displays the cloud top pressure in the sensitive area and figure 9 for the whole data set. 143 simulated IASI pixels are included in the sensitive area, which is located over sea, south-east of Newfoundland. A wide part of the cloud top is located in low-levels in the sensitive area. In that case, the sensitive area is located in the northern exit area of a upper-level jet-streak (Fig. 9). The corresponding distribution of the cloud top level is presented in Figure 10. In the sensitive area, about 40% of the cloud top height are included in the range 1000-900 hPa and only 20% of clouds top level is located above 600 hPa. For the whole data set, the cloud top height is mainly located below 600 hPa. Both synoptic cases shown in the previous subsections exhibit that the cloud cover in the sensitive area varies from case to case. On the contrary, the cloud top level over a wide region of mid-latitude seems almost constant mainly with low-level clouds.

4.3 Averaged results on 8 FASTEX IOPs

Same studies as previously have been conducted for eight cases. The overall forecast range is mostly 36 hours and the verification area is located off-shore western Europe. Often, the sensitivity maximum is located below or at 700 hPa level. The averaged result of the distribution of the cloud top pressure

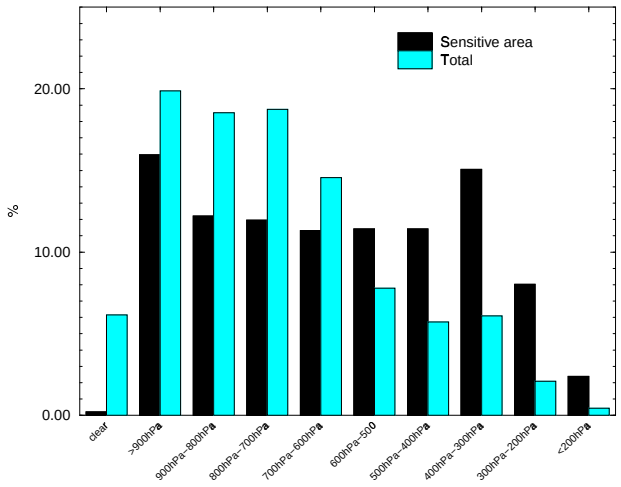

Figure 11: Distribution of the cloud top level of the IASI pixels averaged over the sensitive areas of the 8 FASTEX Intensive Observing Periods and the whole data set corresponding to a mid-latitude region.

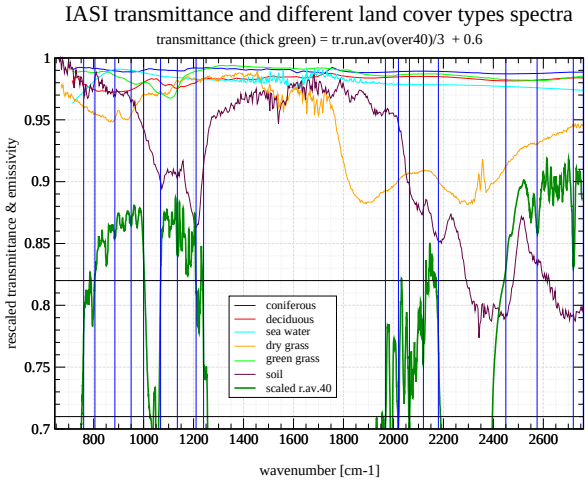

Figure 12: Emissivity spectra for various soil types and averaged transmittances for IASI

is presented in figure 11. While the results of the case studies are shown for the whole data set representative of a mid-latitude region (large amount of cloud top pressure located below 600hPa) as already observed in the 2 IOP shown previously, some differences appear for the distribution of the cloud top pressure in the sensitive area. Two maxima in the distribution of the cloud top level are identified at 1000-900hPa (low-level cloud) and in the layer 400-300 hPa. The consequences for the retrieval of information is that for 20% of the sensitive area, one can assume to retrieve information above the low-level cloud and for about 60% of the sensitive area, one can have some information about the tropopause.

5 LAND EMISSIVITY

To get all the benefit from the assimilation of advanced sounder data over land, it is necessary to have a good knowledge of surface parameters such as surface temperature and emissivity. For the surface temperature, one estimate can be provided by the short-range forecast of a NWP model. For spectral emissivities, these depend on the soil and vegetation types, and also of the vegetation percentage in a pixel. Spectrally varying emissivities have been computed for 18 surface types used as climatological input to the NWP model. They are split into 18 spectral bands, relatively homogeneous from a transmittance point of view. Values were obtained from the MODIS library. The spectral variation of emissivity is presented for a few soil types in Fig. 12. These values are being validated for a given spectral band with MODIS emissivity values.

6 AIRS MONITORING

In summer 2002, a first day of AIRS data has been provided to NWP centres to start testing their software before routine observations become available. A plot of these first orbits is shown in Figure 13. Monitoring is being set up, with the comparison of observations and simulated radiances from the model using the RTTOV radiative transfer model. Different cloud detection modules are also being tried.

7 SUMMARY AND PERSPECTIVES

Advanced infrared sounders will provide thousands of radiance data at every observation location. This number of individual pieces of information is not tractable in an operational NWP context and we have investigated the possibilities of choosing an optimal subset of data to be inserted in the assimilation. The iterative method proposed by Rodgers (1996) has

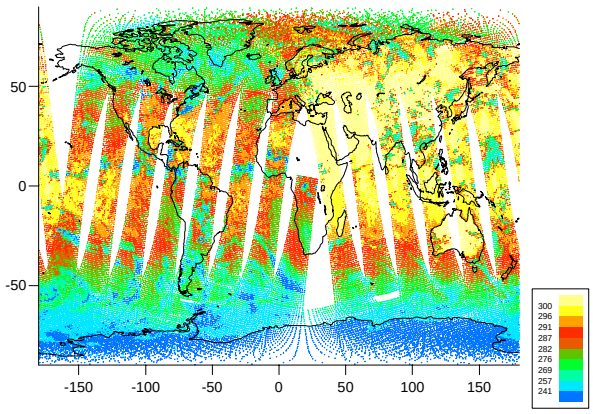

Figure 13: AIRS Brightness temperatures. Date: 20th July 2002.

been extended to a "constant" version. Validation with AIRS NRT set has shown that, although the constant set provided by the iterative method leads to a larger entropy reduction and a larger DFS, the averaged results in terms of analysis accuracy are quite comparable.

An obvious limitation of a constant "optimal" channel selection is that the information content is known to depend on cloud amount (Eyre, 1990) and on surface characteristics. We have started to address the question of retaining the most information possible in sensitive atmospheric structures leading to major forecast failures (Rabier et al.,1996). A study of cloud amount and levels of clouds in the sentitive areas for FASTEX cases has been performed using AVHRR information. Sensitive areas, generally located in the low and mid-troposphere are found to be broadly covered by clouds, reducing the gain of IR sounders for these atmospheric regions. In parallel, the question of getting appropriate a priori information on surface characteristics is being investigated. A correspondance between land types in the NWP model and surface emissivity spectra is being built and validated. Finally, operational centres are preparing to get ready for the assimilation of AIRS data. The Day 1 processing will most likely be the assimilation of less than 300 channels in clear sky situations only. But it is expected that work on cloudy radiances will progress to allow the use of more advanced sounder data, including cloudy ones.

ACKNOWLEDGEMENTS

The authors thank Gwenaelle Hello and Tiphaine Labrot who have provided the sensitivity fields and the cloud parameters of IASI data. Fernand Karcher and Raymond Armante are acknowledged for providing respectively the SODA atmospheric profile database and the mean IASI transmittance on the TIGR database.

REFERENCES

Chevallier F., Chédin A., Chéruy F and J-J. Morcrette, 2000 : TIGR-like atmospheric profile databases for accurate radiative flux computation, *Q. J. R. Meteorol. Soc.*,**126,** 777–785

Collard A.D., 1998 : Notes on IASI performance, *NWP Technical Report No. 253, Met Office, Bracknell, UK*

Desroziers, G., Hello, G. and J-N. Thépaut, 2002 : A 4D-Var Re-analysis of the FASTEX experiment, *Q. J. R. Meteorol. Soc.*,submitted

Eyre J.R., 1990 : The information content of data from satellite sounding systems: A simulation study, *Q. J. R. Meteorol. Soc.*,**116,** 401–434

Fourrié N. and J-N. Thépaut 2002 : Channel selection for AIRS radiance assimilation, *Visiting Scientist Mission Report, available from EUMETSAT*

Hello, G., Lalaurette, F. and J-N. Thépaut, 2000 : Combined use of sensitivity information and observations to improve meteorological forecasts: A feasability study applied to the 'Christmas Storm' case, *Q. J. R. Meteorol. Soc.*,**126,** 621–647

Joly, A. and Collaborators, 1999 : Overview of the field phase of the Fronts and Atlantic Storm-Track EXperiment (FASTEX) project, *Q. J. R. Meteorol. Soc.*,**125,** 877–946

Lavanant L., Legléau H., Derrien M., Levasseur S., Monnier G., Ardouin L., Brunel P. and Bellec B. 1999 : AVHRR Cloud Mask for Sounding Applications, *Proceedings of the Tenth International TOVS Study Conference, Boulder, Colorado, 27 January-2 February 1999*

Matricardi and Saunders, 1999 : A fast radiative transfer model for Infrared Atmospheric Sounding Interferometer radiances, *J. Appl. Optics*, **38,** 5679–5691

McNally, A. 2000 : The occurence of cloud in meteorologically sensitive areas and the implications for advanced infrared sounders. *Proceedings of the Eleventh International TOVS Study Conference, Budapest, Hungary, 20-26 September 2000, 251-255*

Prunet, P., Thépaut, J.-N. and Cassé, V., 1998 : The information content of clear sky IASI radiances and their potential for numerical weather prediction, *Q. J. R. Meteorol. Soc.*,**124,** 211–241

Rabier, F., Klinker, E., Courtier, P. and Hollingsworth, A., 1996 : Sensitivity of forecast errors to initial conditions, *Q. J. R. Meteorol. Soc.*,**122,** 121–150

Rabier F., Fourrié N., Chafaï D. and Prunet P., 2002 : Channel selection methods for infrared atmospheric sounding interferometer radiances, *Q. J. R. Meteorol. Soc.*, **128,** 1011–1027

Rodgers, C. D., 1996 : Information content and optimisation of high spectral resolution measurements, *Optical Spectroscopic Techniques and Instrumentation for Atmospheric and Space Research II*, **SPIE, Volume 2830**, 136–147

Rodgers, C. D., 2000 : Inverse methods for Atmospheres: Theory and Practice, *World Scientific Publ., Singapore*, 238pp